# The Sensitivity of the General Circulation to Arctic Sea Ice Boundaries: A Numerical Experiment

GERALD F. HERMAN

*Department of Meteorology, University of Wisconsin, Madison 53706*
*NASA Goddard Space Flight Center, Greenbelt, MD 20771*

WINTHROP T. JOHNSON

*Sigma Data Services, NASA Goddard Space Flight Center, Greenbelt, MD 20771*

(Manuscript received 28 July 1978, in final form 13 September 1978)

ABSTRACT

A series of experiments were conducted with the Goddard general circulation model to determine the effect of variation in the location of Arctic sea ice boundaries on the model's mean monthly climatology. A control was defined as the mean of six January–February simulations with ice boundaries corresponding to climatologically minimum ice cover occurring simultaneously in the Davis Strait, East Greenland Sea, Barents Sea, Sea of Okhotsk and Bering Sea. An anomaly was similarly defined as the mean of two simulations with maximum ice conditions occurring simultaneously in the same regions. The extremes were estimated from 17 years of observed conditions in the Atlantic sector, and from five years of data in the Pacific sector.

When sea ice boundaries were at their maximum extent the following differences resulted in the January–February climatology as compared with minimum boundaries: Sea level pressure was higher by as much as 8 mb over the Barents Sea, by more than 4 mb in Davis Strait, and by slightly less than 4 mb in the Sea of Okhotsk. Pressure was lower by as much as 8 mb in the north Atlantic between Iceland and the British Isles, and in the Gulf of Alaska. Pressure rises of as much as 4 mb in the eastern subtropical regions of the North Atlantic and North Pacific accompanied pressure falls in the Gulf of Alaska and Icelandic region. Pressure also increased over the Mediterranean region. Geopotential heights at 700 mb were more than 80 gpm lower in the Gulf of Alaska, and more than 100 gpm lower in the Icelandic region. Changes of opposite sign occurred over the subtropics. Zonally averaged temperatures were cooler by 2°C below 800 mb between 50 and 70°N with little change elsewhere. The poleward flux of total energy was a maximum of 13% greater between latitudes 40 and 53°N.

The computed 700 mb geopotential differences were more than twice the inherent variability or "noise" of the model over a broad region of the North Pacific, and between Iceland and the British Isles. Pressure differences were more than twice the inherent variability in the Davis Strait, Gulf of Alaska and Barents Sea, and in the eastern subtropical Atlantic and Pacific. Statistical significance of zonally averaged differences was largest between 50 and 70°N where the confidence levels were as follows: for geopotential height differences, 99% (850 mb), 99% (700 mb) and 97% (500 mb); for temperature, 97% (850 mb) and 92% (700 mb); and sea level pressure, 94%. Confidence levels were high for changes in the Azores region.

On the basis of model results we conclude that ice margin anomalies are capable of altering local climates in certain regions of the high and mid-latitudes. Possible interactions between high latitudes and subtropical regions also are suggested.

## 1. Introduction

Are interannual variations of the wintertime ice cover in the seas of the North Atlantic and North Pacific responsible for any significant changes in large-scale circulation features? Large excursions about the mean limit of the Arctic pack ice boundary are commonly observed in the Barents and Greenland Seas, the Davis Strait, the Sea of Okhotsk and the Bering Sea. Table 1 shows the mean values, extreme limits and standard deviations of the ice extent for the winter months of January–March for the period 1961–77 in the North American and Eurasian sectors. The difference between the extremes can be greater than the approximate area of the average total ice cover, as in the Davis Strait and Labrador Sea.

The predominant effect of ice-cover variation is to alter the exchange of heat and moisture between the atmosphere and the surface of the ocean. This is due to the strong insulating property of a sufficiently thick layer of sea ice. As an example of the large difference in sensible heating between ice-covered and open ocean, Vowinckel and Taylor (1965) computed a surface sensible heat flux of about 220 W $m^{-2}$ over open water for January in the west Eurasian Arctic, as compared with a value of about



0027-0644/78/1649-1664$08.00

TABLE 1. Sea ice cover* in the Atlantic sector, 1961–77 ($10^6$ km$^2$).

| | Average cover | Standard deviation | Maximum | Minimum |
|---|---|---|---|---|
| Davis Straits and Labrador Sea | 0.76 | 0.23 | 1.28 (Feb 1972) | 0.15 (Jan 1974) |
| East Greenland Sea | 1.09 | 0.18 | 1.52 (Feb 1967) | 0.83 (Jan 1972) |
| Norwegian-Barents Sea | 1.42 | 0.16 | 1.82 (Mar 1966) | 0.99 (Jan 1965) |

* Obtained from the *Monthly Ice Charts* of the British Climatological Service, Bracknell.

$-3$ W m$^{-2}$ over ice in the same region. There is an additional effect on the radiation balance due to the larger albedo of ice as compared with ocean, but it is of secondary importance during the winter because the insolation at high latitudes is so small.

There have been many attempts to determine the relationship between local synoptic features and year-to-year variations in the sea ice margin. Because variations in sea ice are themselves forced by atmospheric and oceanic parameters, it has been difficult to prove unambiguously whether an atmospheric feature that correlated with an ice anomaly was the cause rather than an effect of the anomaly. For example, the early work of Brennecke (1904) and Meinardus (1906) showed that colder than average temperatures at Icelandic stations were associated with more southerly boundaries of the pack ice in the East Greenland Sea. Were the colder temperatures the result of the southerly extension of the ice, or were both the ice limits and cold air advection a consequence of the large-scale atmospheric pressure distribution?

There were many subsequent efforts to show that sea ice was the cause of climatic variation. On the basis of ice extent and meteorological data collected at the end of the nineteenth century, Hildebrandsson (1914) hypothesized that average wintertime conditions in Europe and, in fact, throughout the Northern Hemisphere, depended on the summer ice content of the East Greenland Sea. Wiese (1924) found correlations between the ice margin in the East Greenland and Norwegian Seas and subsequent storm frequency and precipitation over northern Europe and Scandinavia. Severe ice in the April–July period was associated with a more southerly track of North Atlantic cyclones during the fall. Wiese also found a good correlation between the mean air temperature in the May-June period in northern Europe and concurrent ice conditions in the Barents Sea. Scherhag (1936) argued that the anomalously warm temperatures at North Atlantic stations during 1932–35 winters were connected with the recession of the ice margin in the East Greenland Sea. Defant (1961, p. 283) suggested a positive feedback between ice extent and atmospheric pressure: southerly ice drift associated with positive pressure anomalies over the polar oceans causes an expansion of the ice margin and a further increase in surface pressure. Ice margin was thus viewed as a mechanism for perpetuating high pressure anomalies in the central Arctic.

There have also been attempts to relate Arctic sea ice to global-scale weather features. Walker (1947) found weak correlations between ice content of the Newfoundland region of the western North Atlantic, and Icelandic and north European pressures, but found no convincing relationships for ice in the East Greenland or Barents Seas. On the other hand, the recent analyses of Schell (1956, 1970), which used more extensive sea ice and meteorological data, have shown some correlation between ice margin and temperatures and pressures over Europe both for concurrent and for time-lagged fields. Schell (1964) conducted a similar study using ice data from a single station in northern Japan but found no significant correlation with subsequent North Pacific pressures.

Recent attempts to predict ice drift in the Alaskan Arctic with empirical orthogonal functions have suggested that there is a correlation between the dominant temperature and sea ice eigenvectors at a time lag of minus one month (cf. Walsh, 1979, Fig. 7). We infer from this that sea ice may cause atmospheric anomalies in the Alaskan Arctic because heavy ice in the Bering and Beaufort Seas leads to colder temperatures in the Alaskan sector one month later.

There has also been speculation concerning the consequences of catastrophic variations of Arctic sea ice, *viz*, the complete removal of the pack ice (cf. Fletcher, 1968) or the extreme ice surges of an ice age (cf. Williams *et al.*, 1974). Fletcher suggested on the basis of heat budget arguments that a hypothetical ice-free Arctic would cause weaker meridional temperature gradients and a weaker zonal circulation, and would be accompanied by more high-latitude snowfall due to increased evaporation over the Arctic Ocean. The Williams *et al.* January simulations with the NCAR general circulation model (GCM) found that ice age boundary conditions caused no significant difference in mean zonal wind strength as compared with the present, but there was a significant southward displacement of the Aleutian and Icelandic lows and the track of maximum midlatitude cyclone activity. However, it is not possible to isolate sea ice effects in this experiment because sea surface temperature, snowline and other boundary conditions were changed along with ice margin.

The early GCM experiments of Fletcher *et al.* (1971) and of Warshaw and Rapp (1973) confirmed the importance of sea ice in high-latitude climate but showed little hemispheric or global influence. Statistical validity of sea ice experiments was established in the Warshaw and Rapp experiments, and

the model results suggested that the stronger convective heating occurring in a hypothetical ice-free central Arctic would give rise to warmer temperatures in the lower troposphere north of about 55°N. The Fletcher *et al.* experiments showed that the complete removal of Arctic sea ice would cause the wintertime anticyclone in the central Arctic to be replaced by a deep low.

Herman and Johnson (1979) conducted a set of experiments to test the sensitivity of the Goddard GCM to extreme variations of sea ice margin in the North Atlantic and North Pacific Oceans. Margin variations nearly twice as large as those observed in recent times were imposed to ensure that there would be a significant difference between calculations carried out for minimum ice conditions, and maximal extent that perhaps represented ice age conditions. The important effect that ice margin had on the mass field (i.e., height of geopotential surfaces) was seen in the Aleutian and the Icelandic regions: 500 mb geopotential heights were as much as 120 gpm lower in the north Pacific corresponding to extreme ice margin changes in the Sea of Okhotsk and Bering Sea.

Here we report the results of a set of numerical experiments conducted with the Goddard (formerly GISS) general circulation model. The experiments were designed to test the model atmospheric response to a single fixed and specified parameter, the total ice cover in the Davis Strait, Barents Sea, East Greenland Sea, Sea of Okhotsk and Bering Sea. Ours differ from any earlier GCM ice experiments by considering margin variations that are substantially smaller than those involved in ice age or ice-free Arctic simulations. Variations imposed here represent approximately the observed conditions during the past 17 years in the three peripheral Arctic seas of the Atlantic sector, and during the years 1973–77 in the Pacific sector. The experiment *control* was the mean of six model calculations with identical ice boundary conditions corresponding to a climatological minimum, but differing from one another by small, random values in the initial temperature, pressure and wind fields. We are required to define our control in this fashion to ensure statistical significance of results (see Appendix B). Similarly, the *anomaly* was the mean of two runs corresponding to climatological maximum sea ice conditions.

The differences that we obtain between the respective means of the control and the anomaly represent to a high level of statistical significance the effect of ice boundary conditions on the *model calculations*. However, there is an important constraint in our model which limits the conclusions we may draw about the effect of sea ice on the true *atmospheric* circulation. Ocean temperatures and sea ice extent are fixed parameters in the model experiments, while their actual evolution is coupled closely to atmospheric processes. Large heat loss from ice-free margin regions could not continue indefinitely. Ocean temperatures would fall and heat

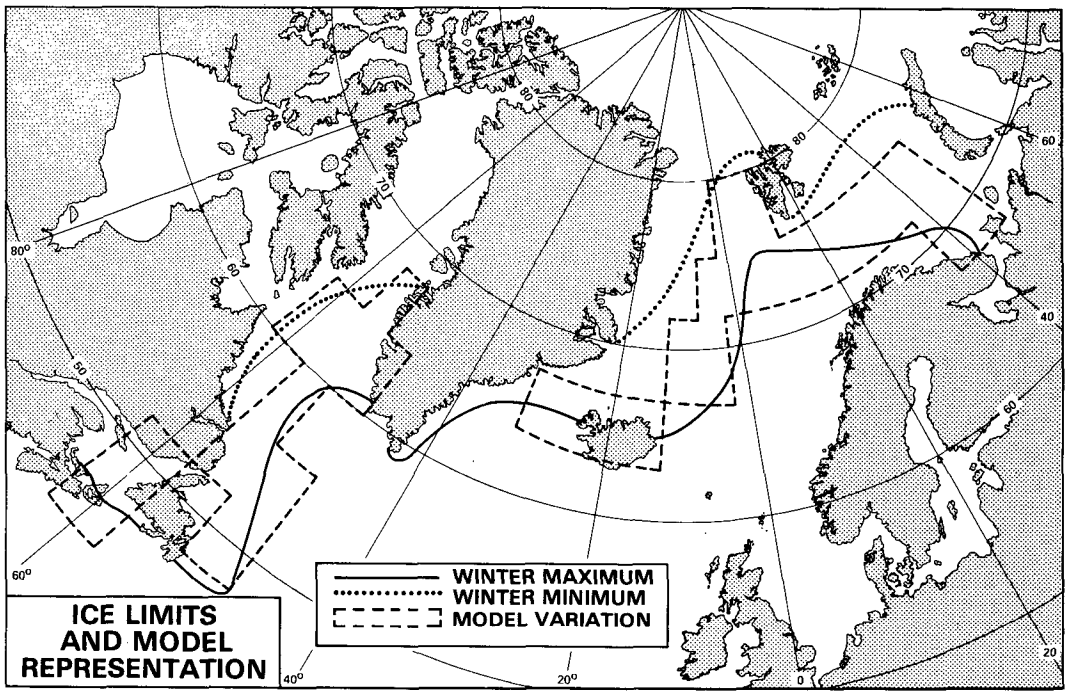


FIG. 1. Composite January–February–March sea ice maxima and minima for the North Atlantic, 1961–77. Dashed line is the Goddard GCM grid representation of the envelope of wintertime ice margin extremes.

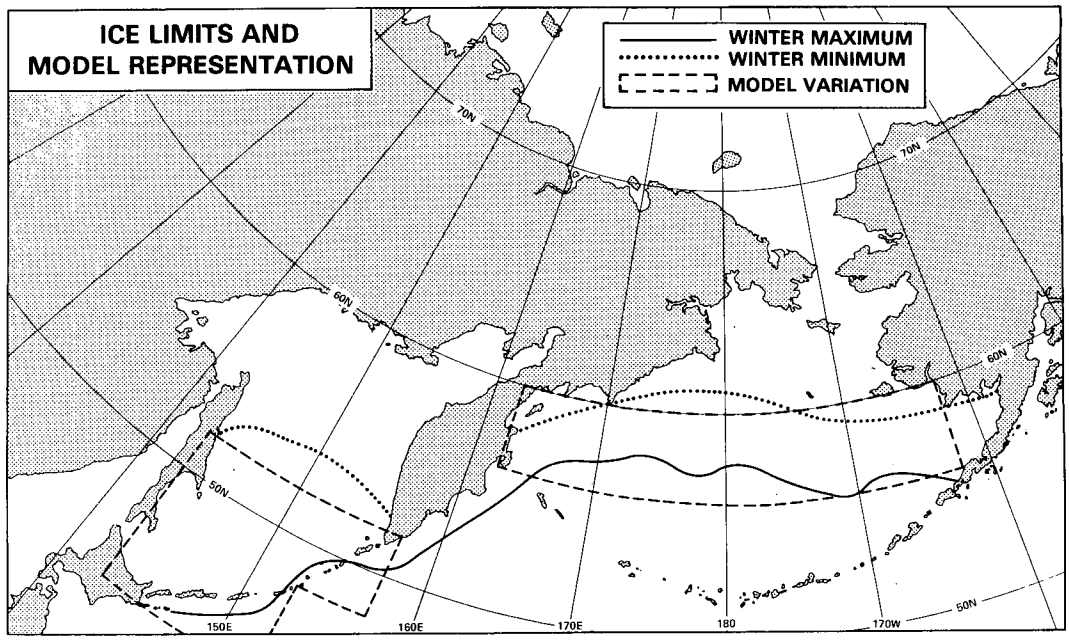


FIG. 2. As in Fig. 1 except for the North Pacific, 1973–77.

flux would diminish. A new layer of ice might even be sustained. For the simulation of monthly climate, however, fixing ice margin is less serious than fixing the sea surface temperature since actual month-to-month margin changes normally are smaller than the changes that occur from one year to the next.

## 2. Design of experiment

### *a. Ice specification*

We have estimated the minimum and maximum extent of sea ice in the Davis Strait and Barents and East Greenland Seas based on the monthly ice charts available from the British Climatological Service, which date to 1961. Shown in Fig. 1 are the approximate maximum and minimum limits for 6/10 to 10/10 pack ice for the years 1961–77 for the composite January–February–March period.

The ice boundaries shown in Fig. 1 represent an *envelope* of extreme ice conditions over the 17-year period. Ice margin does not in general vary synchronously in all Arctic seas, and it is commonly observed (Sanderson, 1975) that maximum conditions in one region of the Arctic accompany minimum conditions in another.

Ice margin limits in the Bering Sea and Sea of Okhotsk determined on the basis of charts from the U.S. Navy Fleet Weather Facility are shown in Fig. 2. Availability of data in the North Pacific constrained us to a smaller number of seasons than in the North Atlantic. The true envelope of extreme conditions in the Pacific would probably be larger if we considered 17 years as we did in the Atlantic. Maximum ice conditions in most seas usually occur during March or April, although April limits were not considered in this experiment.

The rectangular regions in Figs. 1 and 2 represent the model grid areas in which the lower boundary was changed from ocean to ice corresponding to the difference between maximum and minimum conditions. The areal extent and number of grid points are, respectively: Barents Sea, $0.7 \times 10^6$ km$^2$ (9½ points); East Greenland Sea, $1.0 \times 10^6$ km$^2$ (13½ points); Davis Strait, $1.4 \times 10^6$ km$^2$ (10 points); Bering Sea, $0.9 \times 10^6$ km$^2$ (7 points); Sea of Okhotsk, $0.8 \times 10^6$ km$^2$ (5 points). One point in the Great Lakes and two in the Gulf of Bothnia were also changed.

Sea ice in the Goddard model is fixed as a 3 m slab with specified thermal and conductive properties. Sea ice influences the surface energy balance through its temperature, which is calculated from a surface energy balance equation involving net radiative, sensible and latent heat fluxes, heat conduction from the ocean and rate of melting. Its albedo is fixed at 0.70, and evaporation is computed assuming unit ground wetness. Variable ice concentration is not considered, and ice occupies the entire 4° latitude by 5° longitude grid element. All sea ice properties are constant throughout the central Arctic and peripheral Arctic seas.

### *b. Other data specifications*

Model initial conditions were obtained from the 0000 GMT global National Meteorological Center

(NMC) analysis for 1 January 1975. This date was chosen so that recent model statistics could be combined with the earlier initial state perturbation experiments of Spar *et al.* (1978). The distribution of sea surface temperature and Antarctic ice conditions for the control followed closely the Rand Corporation analysis used in the extreme ice experiment of Herman and Johnson (1979).

### *c. Model calculations*

The version of the Goddard model used here is essentially that described by Somerville *et al.* (1974) and Stone *et al.* (1977). Minor modifications that were made subsequent to these papers are briefly summarized in Appendix A.

A single realization of a January–February climate was simulated by integrating the model from 1 January initial conditions until 14 February. Model output at 12 h intervals (0000 and 1200 GMT) was averaged for the period 14 January–12 February. The first 14 calculated days did not enter the average because their fields have larger variances associated with the model's adjustment to initial conditions.

The ensemble mean control (i.e., minimum ice conditions) was estimated as the arithmetic average of six January–February realizations. The first consisted of 1 January 1975 initial conditions, and three others were obtained from the Spar *et al.* (1978) initial state experiments (see Appendix B). Two more runs were added to the ensemble using 1 January 1975 initial conditions but containing several trivial coding differences. The ensemble mean anomaly (i.e., maximum ice conditions) was estimated as the mean of two January–February realizations. One consisted of 1 January 1975 initial conditions but with maximum ice imposed. The second also had maximum ice, but initial temperature, wind and surface pressure that differed by small random amounts as described in Appendix B.

All *difference fields* referred to hereafter will represent the difference between the estimated ensemble mean control field, and the ensemble mean anomaly field, i.e., the average of six runs for minimum ice conditions minus the average of two runs for maximum ice conditions.

## 3. Results of calculation

### *a. Hemispheric fields*

#### 1) Sea level pressure

The distribution of the difference (minimum minus maximum) of mean January–February sea level pressure is shown in Fig. 3. When ice is at its maximum extent in the North Atlantic, sea level pressure rises in the Barents Sea and in Davis Strait, and falls in the North Atlantic between Iceland and Great Britain. Maximum ice in the North Pacific causes a less pronounced pressure increase in the Sea of Okhotsk, and a 4 mb pressure fall in the Gulf of Alaska. The pattern of sea level pressure difference is straightforward to explain. When sea ice covers the Sea of Okhotsk, Barents Sea or Davis Straits, there is much less sensible and latent heating of the atmosphere than there would be if these seas were ice free. Less boundary layer heating results in less low-level convergence and generation of cyclonic vorticity, and leads to a comparatively higher pressure. Although there are no variations of sea ice in the Gulf of Alaska or between Iceland and Great Britain, sea level pressures over these seas were generally lower when ice margin was maximal. Lower pressure northwest of Britain accompanies high pressure in the Barents Sea and Davis Strait as a result of mass conservation. The more difficult question to explain is why the compensating pressure change occurs preferentially in the North Atlantic and not in some other region such as the central Arctic. It is interesting that several of Schell's (1970, Figs. 11–14) composite pressure differences show a similar pattern of lower pressure over Iceland and northern Scandinavia accompanied by high pressure over the North Atlantic-British Isles for light as compared with heavy ice seasons. Such a comparison is limited, however, because Schell had correlated winter synoptic conditions with ice conditions of the preceding April–September period. There is no time lag in the present study.

Sea level pressure differences in the North Pacific are not as systematically related to ice margin dif-

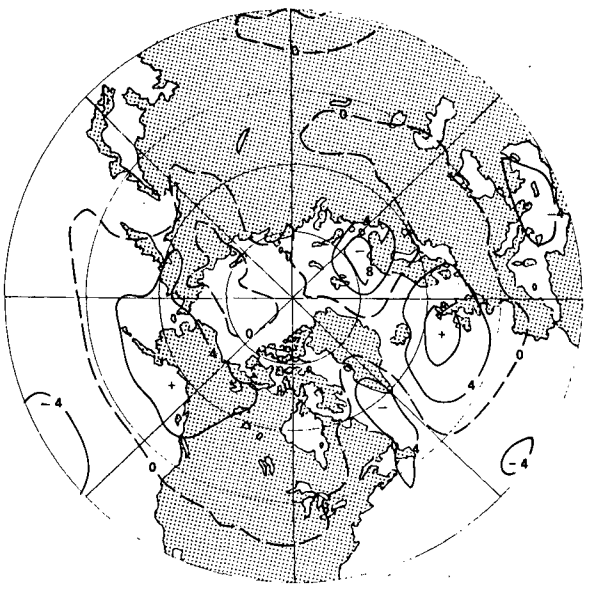

FIG. 3. Sea level pressure difference (mb) corresponding to pressure with minimum (control) ice conditions minus pressure with maximum (anomaly) ice conditions.

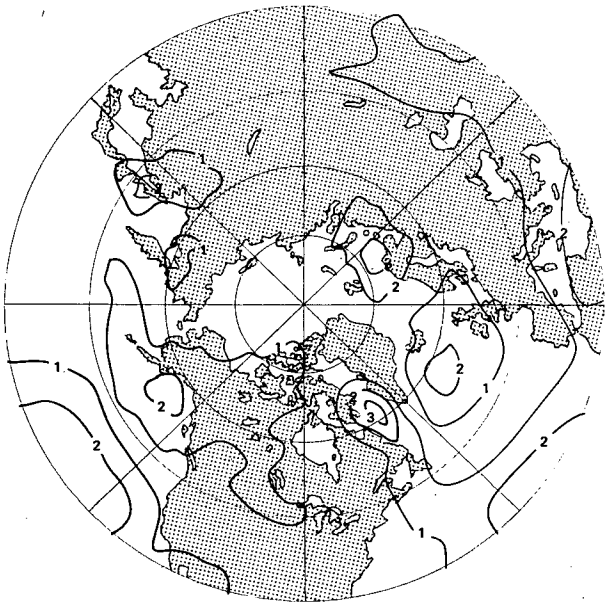

FIG. 4. Ratio of absolute value of sea level pressure difference to standard deviation of sea level pressure.

ferences as they are in the Atlantic. While a pressure rise occurs over the Sea of Okhotsk, pressure has fallen over the Bering Sea and Gulf of Alaska. The Bering Sea differences, however, are not statistically significant. Inherent variability (cf. Appendix B) of the Goddard model is larger in the Bering and Norwegian Seas than anywhere else in the Northern Hemisphere. Pressure differences in the Bering Sea simply are indistinguishable from noise.

As a measure of statistical significance we consider the signal-to-noise ratio which is obtained by normalizing pressure differences by the standard deviation of sea level pressure (Fig. 4). The increase in pressure caused by more ice exceeds two standard deviations of model noise over the Sea of Okhotsk and northern Japan, the Barents Sea and northern Scandinavia, and in the Davis Straits. The compensating pressure falls exceed two standard deviations locally in the Gulf of Alaska, and in the north Atlantic between Iceland and Great Britain. Regions with differences of two standard deviations or more occur also in the eastern mid-Pacific, eastern mid-Atlantic and over North Africa. Differences which occur in the subtropics suggest possible teleconnections between the high latitudes, midlatitudes and subtropical latitudes and are discussed further in Section 3c.

### 2) 700 mb TEMPERATURE AND GEOPOTENTIAL

The model's 700 mb hemispheric temperature field is altered by the imposed ice margin changes (Fig. 5a). Because there is stronger convective and latent heating associated with minimum ice cover, 700 mb temperatures are colder with maximum ice in the Sea of Okhotsk, over the northwestern Soviet Union, and over the north Atlantic between the southern tip of Greenland and the British Isles. These temperature changes with maximum ice cause the 700 mb geopotential height (Fig. 5b) to decrease by more than 80 gpm in the North Pacific, and by more than 100 gpm in the North Atlantic. There is some uncertainty in relating the location

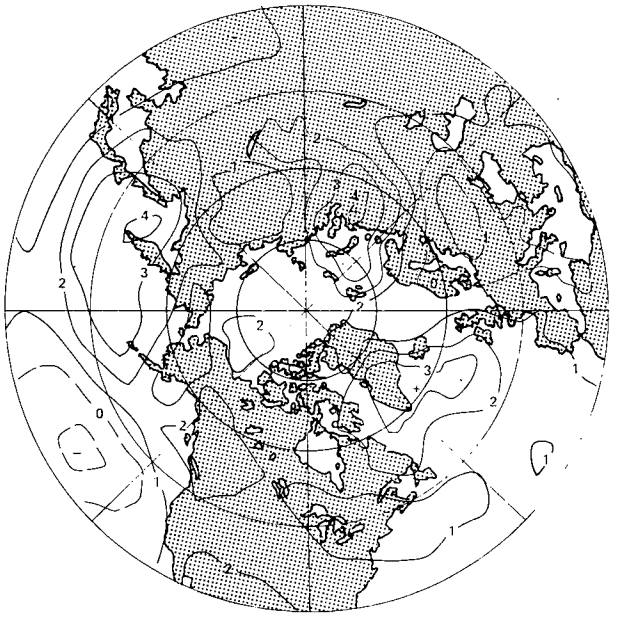

FIG. 5a. 700 mb temperature difference corresponding to minimum minus maximum ice conditions.

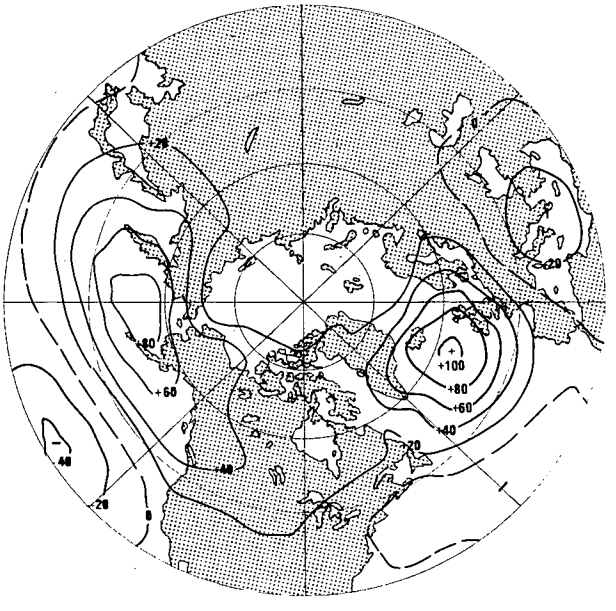


FIG. 5b. 700 mb geopotential height difference (gpm) corresponding to minimum minus maximum ice conditions.

of upper level changes to the location of surface changes because we imposed ice margin changes in several regions simultaneously. The change in the North Atlantic could be a downstream response to changes in the East Greenland Sea. Similarly, the temperature change centered over Novaya Zemlya could be a downstream response to the East Greenland Sea change, or a local response to the Barents Sea change. Here local responses would correspond to virtually no phase lag between the location of the heat source and location of maximum temperature change, while the downstream interpretation would require phase lags of about 30–40° from the heat sources in the Davis Straits and Barents Sea. Positive differences occur also over western Canada and the southwestern United States.

The absolute value of the geopotential difference between minimum and maximum ice conditions is normalized by the standard deviation of the 700 mb geopotential height and is shown in Fig. 6. Differences larger than three standard deviations are obtained to the east of Hokkaido and the Kamchatka peninsula. The differences between Greenland and the British Isles are greater than two standard deviations. Differences over the rest of the Northern Hemisphere are difficult to distinguish from noise.

Ice margin apparently is capable of affecting the pattern of "blocking" in the model's 700 mb flow field. If the surface heat sources (i.e., ice-free areas) are located sufficiently close to the major stationary troughs in the North Atlantic and North Pacific, then the changes in amplitude of both

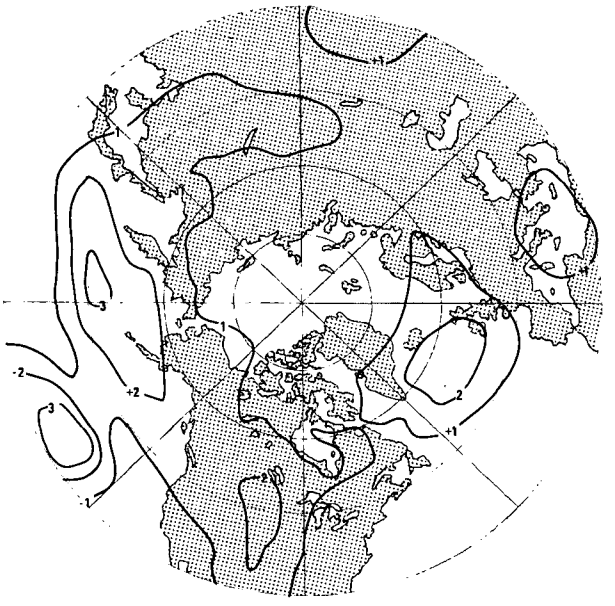

FIG. 6. Ratio of the absolute value of the 700 mb height difference to the standard deviation of the 700 mb height field.

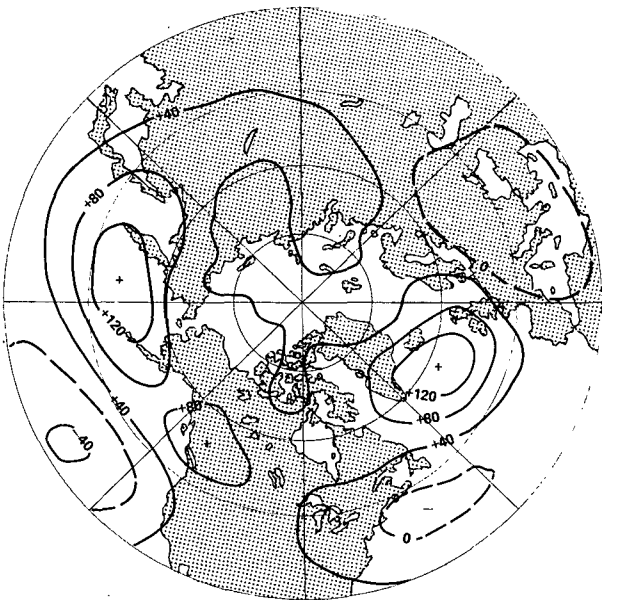

FIG. 7a. 300 mb geopotential height difference (gpm) corresponding to minimum minus maximum ice conditions.

ridges and troughs at 700 mb may become very large due to resonant forcing. Similar effects have been attributed to North Atlantic sea surface temperature anomalies (Namias, 1964) and dynamical mechanisms have been proposed by Smagorinsky (1953) and others.

### 3) 300 mb GEOPOTENTIAL

Geopotential height differences caused by ice margin variation occur at high levels, and do not appear to have any systematic phase shift with height. Figs. 7a and 7b show that large differences and signal-to-noise ratios occur at 300 mb to the east and south of the Sea of Okhotsk, over the central United States, and northwest of Great Britain. The features are similar to those in the 700 mb geopotential difference field, but in the Atlantic and Pacific there is a slight shift southward and eastward of the region of ice margin change. Evidently the largest phase shifts are confined to the lowest 300 mb of the troposphere.

## *b. Zonally averaged temperature*

Differences in the pattern of surface heating due to margin variations have an effect on the zonally averaged temperature, but significant changes are confined to the lowest layers of the high-latitude troposphere. Zonal temperatures (Fig. 8) are 2°C greater with less ice in the belt 42–70°N and from the surface to 800 mb. The corresponding signal-to-noise ratio (not shown) exceeds 2 between 50–70°N up to 600 mb, and exceeds 3 up to 835 mb.

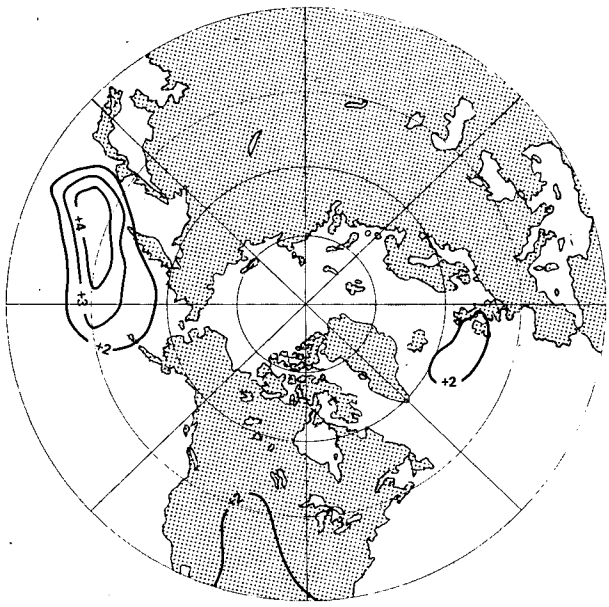

FIG. 7b. Ratio of the absolute value of the 300 mb height difference to the standard deviation of the 300 mb height field.

### c. *Hemispheric changes and teleconnections*

In addition to local changes that occurred at latitudes where the ice margin perturbations were imposed, there were regions of high statistical significance in subtropical latitudes, and even in the Southern Hemisphere. Signal-to-noise ratios larger than 2 occur in the sea level pressure field (Fig. 9) in the eastern subtropical Atlantic and eastern subtropical Pacific Oceans and in the Mediterranean region. Small regions of significance in sea level pressure appear near the Weddell Sea and near the Tasman Sea, but these can be dismissed as being statistically spurious, even if they do represent more than a single point. Some grid points will be significant purely on the basis of chance, and these points will necessarily involve a number of adjacent grid points because the sea level pressure field is spatially coherent, i.e., pressures at adjacent model grid points are related through hydrostatic and hydrodynamic laws. Moreover, it is hard to imagine a viable mechanism that could relate Southern Hemisphere changes to Arctic ice perturbations. [The possibility of relationships between north and south polar ice has been mentioned by Defant (1961).]

There are good reasons for believing that the subtropical changes are real and caused by Arctic ice variations. Regions of significant differences in the subtropics occur systematically between most of the control and anomaly runs, and they cover areas that are as extensive as the differences at high midlatitudes. More importantly, the possibility of a significant relationship between pressure variations in high and low latitudes of the North Atlantic is becoming well established on the basis of observations. Kutzbach (1970) showed that the pattern for the first eigenvector of the January sea level pressure consisted of large variations of opposite sign occurring in the Icelandic region and the mid-Atlantic. Additional evidence that variations in the Icelandic region are accompanied by variations of

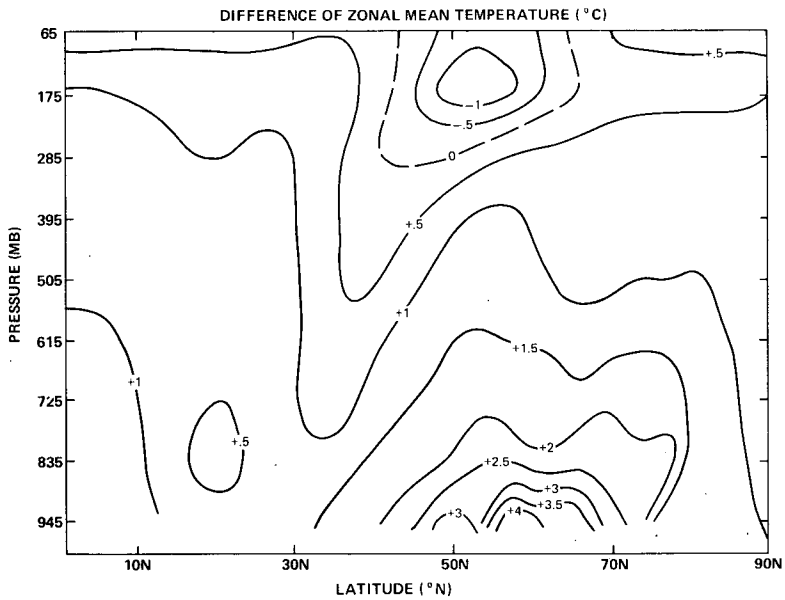


FIG. 8. Difference between zonal mean temperature corresponding to minimum minus maximum ice conditions. Positive values signify that temperatures are colder with maximum ice.

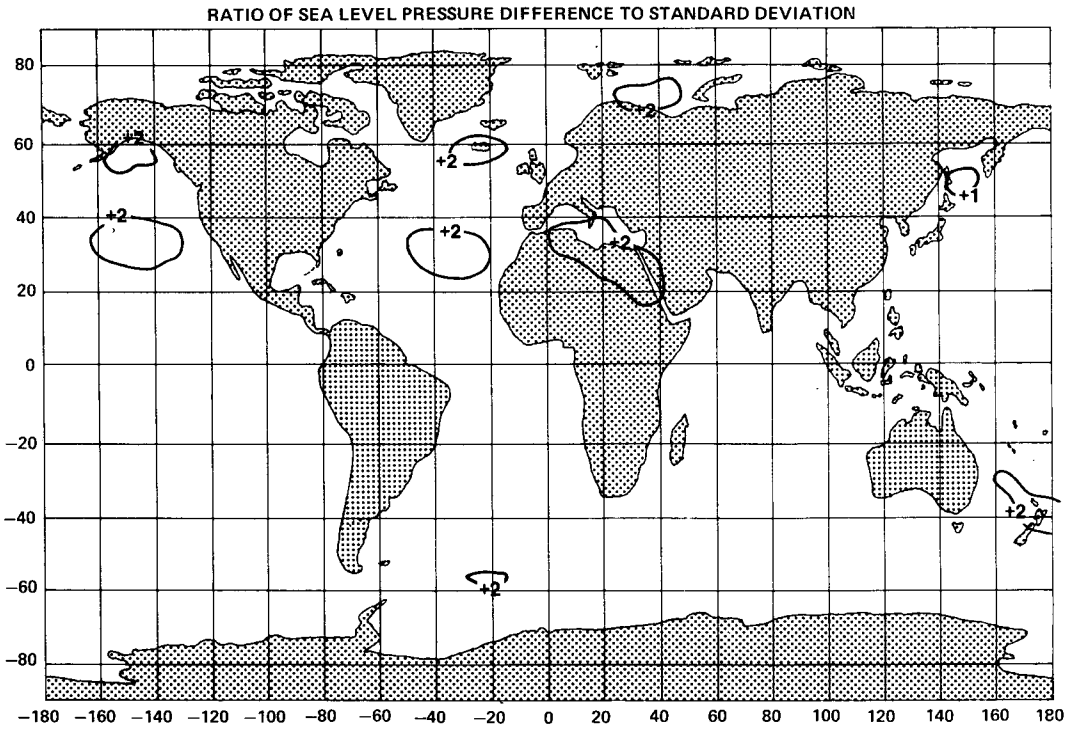


FIG. 9. Absolute value of signal-to-noise ratio for global sea level pressure difference. Values greater than 2 in subtropics correspond to higher pressure with maximum ice, while in the Gulf of Alaska and near Iceland they correspond to lower pressure.

opposite sign near the Azores has been presented in the sea surface temperature (SST) studies of Bjerknes (1962), and has also been mentioned by Lamb (1971). Namias (1972) found that intensification of the Azores High accompanies low-pressure anomalies in the Newfoundland Sea region.

If the results of this experiment are representative of the true atmospheric response to sea ice variations, then they support the hypotheses of Namias (1958) and others that there exist *teleconnections* or physical relationships between anomalies at high latitudes or in the Arctic, and anomalies at lower latitudes. It is not surprising that the pattern of teleconnections for ice anomalies resembles so closely that for SST anomalies (e.g., Namias, 1964; Ratcliffe and Murray, 1970) because both anomalies represent an alteration of the thermal forcing of planetary-scale waves.

We cannot at this time state quantitatively a dynamical mechanism for these concurrent changes. The explanation obviously involves conservation of mass and vorticity. Ice anomalies in the Atlantic occur near 65°N, i.e., close to the rising branch of the wintertime Ferrel cell, which automatically couples the surface convergence near 60°N to that near 30°N, i.e., near the descending branch of the cell. Alternatively, the amplification of the North Atlantic trough through generation of positive vorticity accompanies an intensifying ridge and negative vorticity.

### *d. Integral quantities*

It has been suggested in discussions of long-term climatic effects of sea ice (cf., World Meteorological Organization, 1978, p. 10) that variations in ice extent would change the poleward transfer of heat by the eddies and by the mean meridional circulation. In order to examine possible changes in the poleward flux, we have computed the vertical integral of the zonally averaged total energy flux due to eddies, $F_e$, where

$$F_e = (2\pi a/g)\cos\theta \times \int [C_p(vT)_e + L(vq)_e + (v\Phi)_e]dp, \quad (1)$$

and that due to the mean meridional circulation, $F_m$, where

$$F_m = (2\pi a/g)\cos\theta \times \int [C_p(vT)_m + L(vq)_m + (v\Phi)_m]dp. \quad (2)$$

Here $(vT)_e$ and $(vT)_m$ are the northward temperature fluxes by the eddies and the mean circulation, respectively. Similarly, $(vq)_e$ and $(vq)_m$ are the water

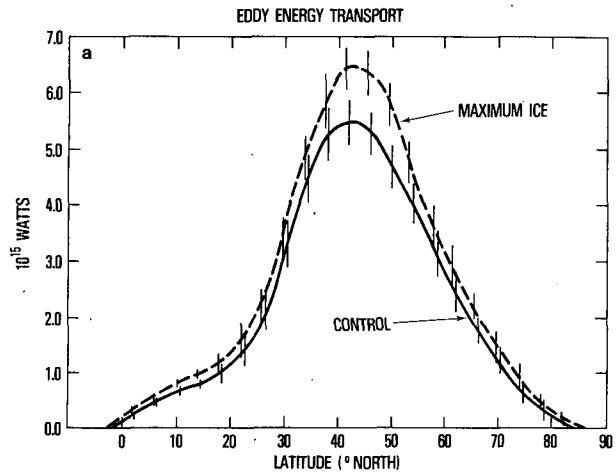


FIG. 10a. Vertically integrated poleward energy flux by eddies.

vapor fluxes and $(v\Phi)_e$ and $(v\Phi)_m$ are geopotential fluxes. Also, $C_p$ is specific heat, $L$ latent heat of vaporization, $g$ gravity, $p$ pressure, $\theta$ latitude and $a$ the earth's radius.

Figs. 10a and 10b show the ensemble mean values of $F_e$ and $F_m$, respectively, for maximum and minimum ice conditions. The error bars on the curves denote the standard deviations of $F_e$ and $F_m$ for the six runs that comprise the control.

Between latitudes 40 and 53°N the eddy energy flux with maximum ice is larger by almost $1 \times 10^{15}$ W, which is more than twice the standard deviation of the energy flux in the control runs. Elsewhere the energy transport is larger, but the differences cannot be considered statistically significant. The magnitude of the energy flux by the mean meridional circulation is significantly larger between 40 and 53°N with maximum ice but differences are trivial elsewhere.

These results suggest that the feedback between sea ice and the poleward eddy energy flux is negative. As the ice margin expands, the temperature gradient at the surface and at low levels is increased and baroclinicity is enhanced. Larger transports result from a combination of a stronger gradient near 50°N and increased eddy activity. Although the real ice margin depends on ocean surface temperature and salinity, which our model does not compute, we speculate that there could be a limit to ice margin growth that is determined by the atmospheric energy transports. That would occur if there were a convergence of heat into the latitude bands where the ice margin was expanding that was large enough to inhibit further growth or even cause recession of the pack ice.

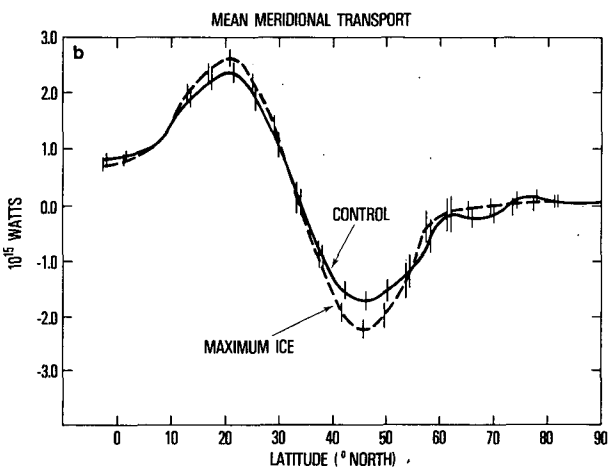


FIG. 10b. Vertically integrated poleward energy flux by mean meridional circulation.

We did not compute the terms in the Lorenz energy cycle for these experiments. In the earlier ice extent experiment (Herman and Johnson, 1978) we found only slight differences in the conversion and storage terms for margin differences that nearly corresponded to ice age conditions.

## 4. Significance of results

The results presented here are clear evidence that variations of the fixed sea ice boundaries in the Goddard GCM cause statistically significant differences in the model's mean monthly climate both in high midlatitudes and in subtropical high-pressure zones. The model's response is consistent with our physical notion of how the atmosphere should respond to changes in surface heating at high latitudes, and these results strongly support numerous hypotheses that there are observed atmospheric anomalies that not only correlate with ice margin variations but are caused by them. In contrast to studying real atmospheric data, there is little ambiguity in determining that changes in the model's circulation were caused precisely by the ice margin changes provided that the circulation changes are sufficiently greater than the inherent model variability. This advantage results from being at liberty to specify fixed ice margins and ocean surface temperatures during the model calculation, but is at the price of neglecting the potential feedbacks between the ice cover and the high latitude heat budget and circulation. The sensible and latent heating over the model's ice-free Arctic seas would not proceed at the same rate in the atmosphere because the real ocean surface layer would lose heat to the atmosphere during air mass modification, and possibly even initiate accretion of new ice. The magnitude of the changes calculated here probably would be smaller if the model included an interactive ocean surface layer and pack ice because the heat fluxes would diminish as the ocean cooled.

If it is assumed that these results represent the true atmospheric response to ice margin anomalies, then several significant implications follow.

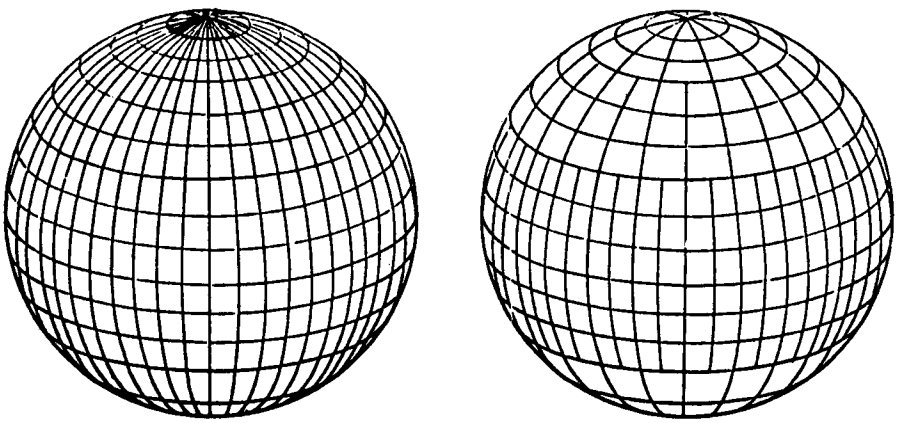

FIG. A1. Split grid as used in GLAS model.

1. *Ice margin is capable of exerting local-synoptic influence*. The Davis Strait, the Barents Sea and the Sea of Okhotsk, and parts of the East Greenland Sea will have higher pressure when they are ice covered and this represents either less frequent or less intense cyclone activity, and concomitant cloudiness and precipitation. At the same time the expansion of the high pressure into the Barents Sea between Norway and Spitsbergen should cause a southward deflection of North Atlantic cyclones as proposed by Wiese (1924) and Schell (1970), but the statistical significance of such a conclusion is not high. We have computed the average precipitation for the control over Scandinavia of $1.6 \pm 0.7$ mm day$^{-1}$, and over northern Europe of $0.8 \pm 0.3$ mm day$^{-1}$. For the anomaly we obtain $2.5 \pm 0.7$ mm day$^{-1}$ over Scandinavia and $1.4 \pm 0.5$ mm day$^{-1}$ over northern Europe. Such an increase in precipitation would be consistent with more north Atlantic cyclones being deflected to northern Europe when there is maximum ice.

If real large-scale ice margin anomalies are sufficiently long-lived, i.e., they persist for a time period comparable to or greater than the length of our averaging period (~4 weeks), then there is predictive value in observing the location of the ice margin. [According to J. E. Walsh and C. M. Johnson (personal communication, 1978) ice margin anomalies tend to persist for several months.] A relatively large anomaly ("signal") would be required because of the large atmospheric variability in high and mid-latitudes. Sea level pressure changes correlate with concurrent ice margin changes, but from the present study we can make no statement about the possibility of time-lagged correlations.

2. *Ice margin is capable of exerting synoptic influence on a hemispheric scale*. Because anomalies of the Azores high have been found to be so well correlated with Icelandic low anomalies, ice margin changes in the Davis Strait or East Greenland Sea are linked to pressure changes in the subtropical regions of the eastern North Atlantic Ocean through their effect on the Icelandic low. The pressure change mechanism in the model involves only atmospheric processes because model sea surface temperatures are specified and do not respond to changing atmospheric conditions. Anomalies of seasonal climate in polar, mid-latitude and tropical regions are interdependent, and the construction of empirical or numerical prediction models as well as the design of observing systems necessarily involve hemispheric considerations.

## APPENDIX A

### Model Considerations

Several features of the Goddard GCM have been changed subsequent to the model summary given by Somerville *et al.* (1974). Those changes which were implemented in our calculations were in the high-latitude differencing scheme and in the parameterization of the planetary boundary layer and ground hydrology.

Differencing schemes containing grid elements equally spaced in latitude and longitude are less desirable because the Courant-Friedricks-Levy (CFL) stability criterion places a severe limitation on the size of the time step because of the spatial convergence of meridians in polar regions. Additional filtering of the highest frequency modes is required at those latitudes where the CFL condition is violated.

In an internal publication Halem and Russell[1] describe the so-called split-grid differencing scheme that is applied at high latitudes. The split grid retains a grid spacing of 4° latitude by 5° longitude up to 62°N. From 66 to 78°N the longitudinal spacing is 10°, and from 82° to the Pole it is 20° (Fig. A1). The modification also is made in the

[1] Goddard Space Flight Center, Institute for Space Studies, 1973 Research Review, pp. 194–200.

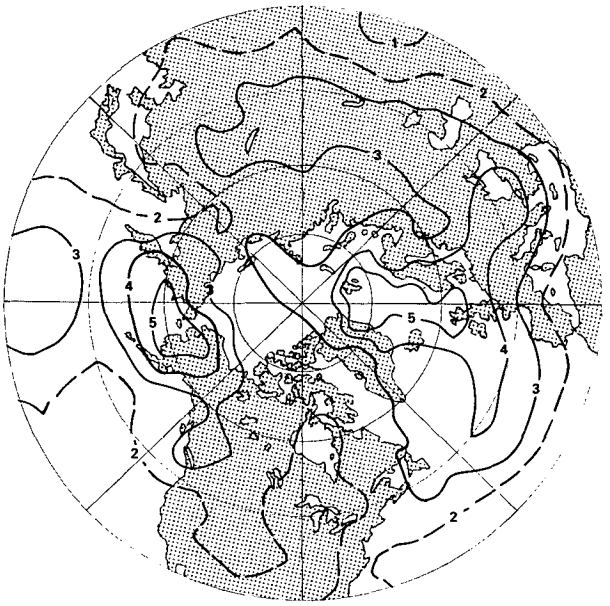

FIG. B1. Standard deviation (mb) of six mean monthly sea level pressure fields used for control.

Southern Hemisphere. The finite-difference equations were constructed for the new mesh spacing to ensure the same quadratic conservation properties of the original Arakawa differencing scheme for equal spacing on spherical grids. Additional differencing modifications to the momentum conservation equation were required to guarantee the conservation properties involving the integrated pressure gradient terms and the Coriolis term. It was found that the integration step could be doubled while eliminating spurious instabilities and significantly reducing the amount of smoothing required in polar regions. Model accuracy was not significantly affected outside of polar regions.

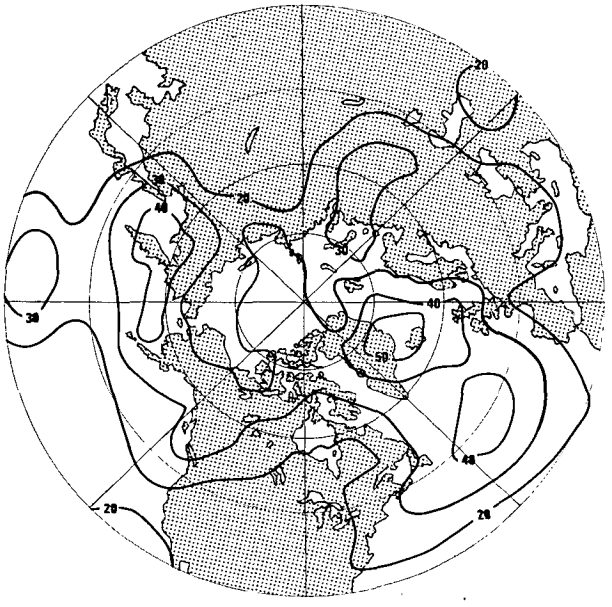

FIG. B2. Standard deviation (gpm) of six mean monthly 700 mb geopotential height fields.

The drag coefficient which governs surface exchange was multiplied by an empirical coefficient to give better agreement with observations. The surface roughness $z_0$ over the ocean is computed as a function of the friction velocity $u_*$. Following Cardone (1969),

$$z_0 = Au_*^{-1} + Bu_*^2 + C, \qquad \text{(A1)}$$

where $A$, $B$ and $C$ are empirically derived constants. The surface roughness enters into a logarithmic law for the drag coefficient which is solved interatively because it involves $u_*$ implicitly.

Ground wetness is fixed globally in the model's hydrology, but the ground temperature calculation includes the temperature change caused by the freezing or melting of ice in the ground. For this reason an account is kept of the fraction of total water that is frozen at each grid point.

## APPENDIX B

### Statistical Evaluation of Results

Do the calculated difference fields represent a statistically significant difference between the mean control (minimum) ice conditions and mean anomaly (maximum) ice conditions? We estimate control and anomaly means as arithmetic averages of six and two January–February simulations, respectively. It is possible that other difference fields could have been generated if other members of a normal population of January–February simulations were chosen to compute control and anomaly means.

Laurmann and Gates (1977) and Chervin and Schneider (1976) have proposed several statistical tests for evaluating GCM model results. Ideally, conclusions reached on the basis of GCM simulations should be independent of the statistical test used. Statistical evaluation of this experiment was based on consideration of signal-to-noise ratios and a Student's $t$-test.

#### *a. Signal-to-noise*

Model "noise" or "inherent variability" is a measure of the extent to which the numerous dynamic instability mechanisms represented in a model amplify small differences in the initial state, or even differences associated with computer round-off. These mechanisms include baroclinic and barotropic instability, layered convective adjustment and parameterization of subgrid-scale cumulus convection. (In nature these are some of the mechanisms that cause one January climatology to differ from another.)

We expanded on the initial state perturbation experiments of Spar *et al.* (1978). The Spar *et al.* experiments specified rms errors in the initial state for 1 January 1975 over land consisting of differences in temperature, wind and sea level pressure of 1°C, 4 m $s^{-1}$ and 3 mb, respectively. These figures were doubled over the oceans. These values represent the standard deviation of a normal distribution of differences specified randomly over land and over the ocean.

The control ensemble mean $\mu_c$ of a quantity $\phi$ is the arithmetic average of the mean value of that quantity obtained in each of $N$ runs, i.e.,

$$\mu_c = \sum_{i=1}^{N} \phi_i/N. \quad \text{(B1)}$$

The mean value $\phi_i$ is the arithmetic average of a model quantity $f_{ij}$ which is sampled every 12 h. Thus, averaging over the last 30 days of a 42.5-day perturbation run,

$$\phi_i = \sum_{j=1}^{60} f_{ij}/60. \quad \text{(B2)}$$

The anomaly ensemble mean $\mu_a$ is similarly defined with $N = 2$. As a measure of noise we use the unbiased estimate of the standard deviation $s$ of the control mean,

$$s = [\sum_{i=1}^{N} (\mu_c - \phi_i)^2/(N-1)]^{1/2}. \quad \text{(B3)}$$

Fig. B1 shows the standard deviation of sea level pressure computed from the six control simulations. The dominant feature of this map is that the largest standard deviations are found in middle and high latitudes, and most notably in regions where ice margin variability is observed to be the largest. This is not surprising since ice margin variations are caused largely by synoptic variations (cf., Walsh, 1978). Variability is largest (≥5 mb) in the extremely baroclinically unstable region off the east coast of Siberia, and in a portion of the North Atlantic storm track along the Greenwich meridian between Scotland and Spitsbergen. Variability of more than 3 mb occurs in the central North Pacific, central North Atlantic, and over most of Europe and central Asia. Values of 2 mb or less occur equatorward of about 38° everywhere except in the central Pacific.

The pattern of variability is qualitatively the same at 700 mb and at 300 mb as the standard deviation of geopotential height surfaces (Figs. B2 and B3) indicate. Two maxima occur over Asia, one directly over the Sea of Okhotsk, and another extending from the Barents Sea along the Ural mountains to central USSR. Maxima also occur in the central North Atlantic and North Pacific, between Greenland and northern Europe, and over northwestern North America.

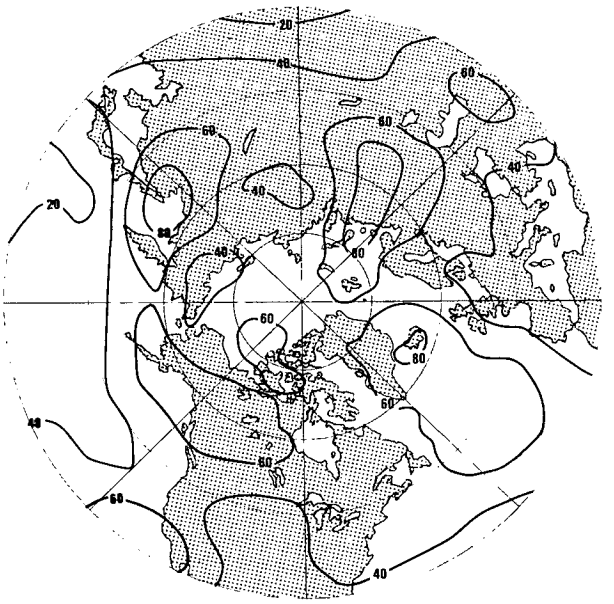


FIG. B3. As in Fig. B2 except for 300 mb geopotential height fields.

*b. "t-tests"*

We have also computed a Student's $t$-test for our results and find that our conclusions are not significantly different from those reached on the basis of signal-to-noise ratios. In particular, the Welch test as used by Chervin and Schneider [1976, Eqs. (2) and (3)] was applied to determine the confidence level at which we reject the hypothesis that there is no significant difference between control and anomaly. Fig. B4 shows the model grid points for which a 95% confidence value was computed for sea level pressure differences. (Individual grid points for which the calculated confidence level was 95% or greater are denoted by a plus sign.) Clusters of points for which the confidence level was 95% or greater for sea level pressure occur in the Gulf of Alaska, Davis Strait and Barents Sea; in the North Atlantic between Iceland and the British Isles, in the eastern regions of the subtropical North Atlantic and North Pacific Oceans; and over North Africa. Values of 95% occur at a number of other isolated points. The significance of 500 mb temperatures is somewhat different where clusters of points having greater than 95% confidence are found only over the North Pacific, the central United States and over the eastern subtropical Atlantic. There are also grid points in the Antarctic with 95% confidence values.

In fact, the $t$-statistic of a variable at a single grid point is not a meaningful quantity because the true sample size includes all global grid points. A better measure of confidence is the $t$-statistic that is computed for geographically averaged quantities.

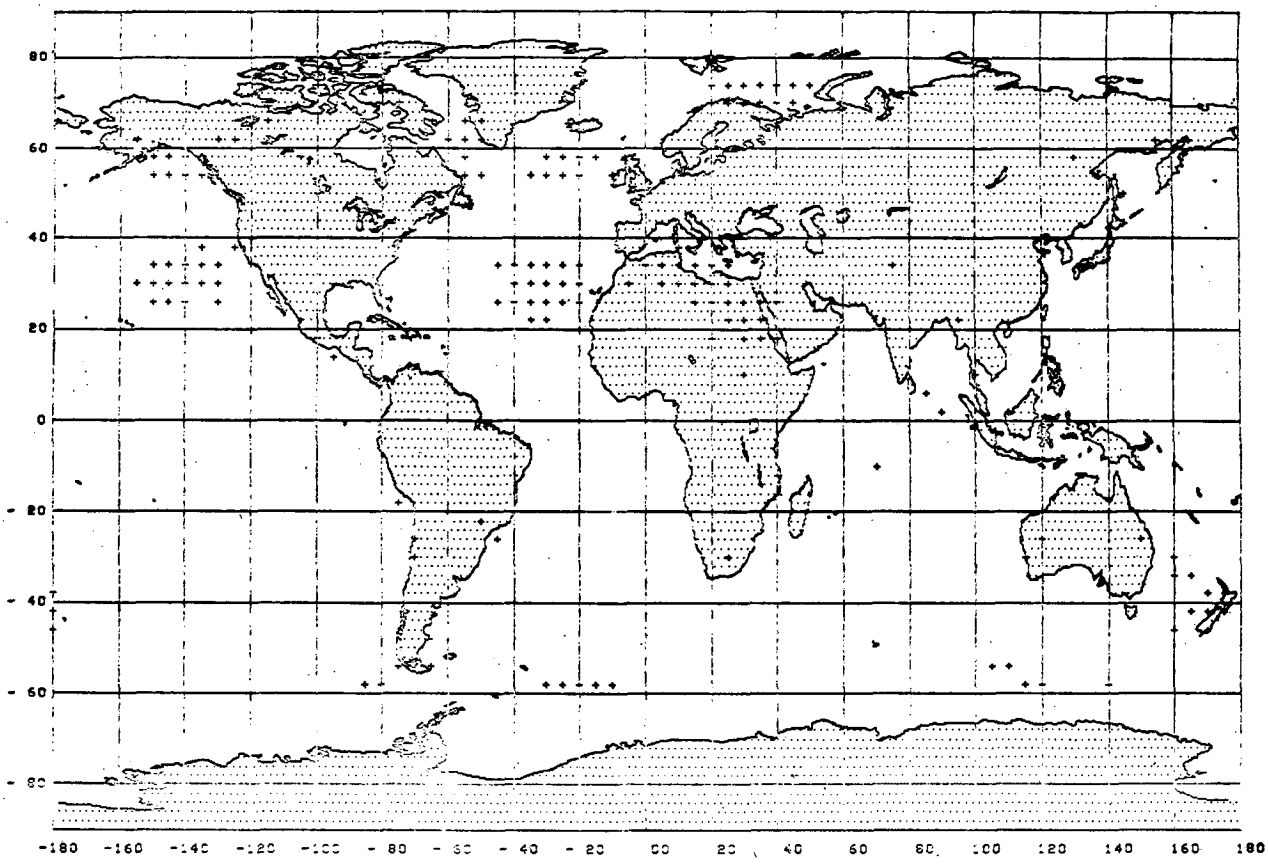


FIG. B4. Global distribution of model grid points at which sea level pressure difference between control and anomaly had a confidence value of 95% or greater (denoted by plus sign).

In Table B1 are shown the confidence levels for differences between ensemble means of areally averaged quantities, e.g., the mean of six average Northern Hemisphere sea level pressures of the control minus two average Northern Hemisphere pressures for the anomaly. Calculations are shown for global and hemispheric averages, averages about 20° latitude bands, and several local regions of interest.

The largest confidence values are found in the 70–50°N latitude band where values of 99% occur in 850 and 700 mb geopotential height, and 94% in sea level pressure. (The largest zonally averaged geopotential and temperature signal-to-noise ratios occurred between 70 and 50°N.) Large confidence values do not systematically occur in any other latitude bands. Note that the confidence value for both globally averaged 850 mb temperature and geopotential difference is 92%. Northern Hemisphere temperature differences have largest confidence values (94%) at 850 mb, and geopotentials (96%) at 700 mb. Hemispheric pressure differences are not significant.

On a regionally averaged basis sea level pressure differences yield high levels of confidence (95%) when averaged over western Canada and Alaska, and over the subtropical north Atlantic ocean. Values for temperature and geopotential differences are generally high when averaged over the North Pacific, but not when averaged over the north Atlantic. (A greater fraction of grid points had large signal-to-noise ratios in the area arbitrarily defined as North Pacific than in the one defined as North Atlantic.) Note that confidence levels are generally low for variables averaged over the central Arctic, northern Europe and Scandinavia.

In general we view these results with some pessimism as they illustrate the difficulty of observing the high-latitude response in GCM sensitivity studies. Relatively small differences in surface and upper level fields yield relatively high confidence levels in tropical and subtropical regions, but relatively large anomalies (ice cover or surface temperature) are required to produce a significant impact on meteorological fields at high latitudes. Clearly, it will be more difficult to predict seasonal fluctuations in high latitudes and midlatitudes based on response to anomalies in lower boundary conditions.

*Acknowledgments*. We are indebted to Dr. Milton Halem and the staff of the Modelling and Simulation

TABLE B1. Confidence level (percent) for differences between geographically averaged quantities.

| | $T_{850}$ | $T_{700}$ | $T_{500}$ | SLP | $Z_{850}$ | $Z_{700}$ | $Z_{500}$ |
|---|---|---|---|---|---|---|---|
| 1. Global average | 92 | 88 | 82 | 80 | 92 | 92 | 90 |
| 2. Northern Hemisphere average | 94 | 91 | 81 | 49 | 94 | 96 | 93 |
| 3. Southern Hemisphere average | 88 | 85 | 82 | 82 | 86 | 86 | 86 |
| 4. Zonal averages | | | | | | | |
| 90–70°N | 94 | 90 | 73 | 7 | 27 | 61 | 76 |
| 70–50°N | 97 | 92 | 74 | 94 | 99 | 99 | 97 |
| 50–30°N | 91 | 86 | 75 | 71 | 17 | 79 | 83 |
| 30–10°N | 89 | 92 | 87 | 89 | 79 | 89 | 90 |
| 10–10°S | 84 | 83 | 84 | 59 | 66 | 90 | 87 |
| 10–30°S | 87 | 84 | 78 | 71 | 10 | 92 | 87 |
| 30–50°S | 80 | 71 | 61 | 69 | 59 | 37 | 18 |
| 50–70°S | 86 | 85 | 83 | 84 | 85 | 85 | 85 |
| 70–90°S | 96 | 88 | 87 | 71 | 77 | 80 | 83 |
| 5. Regional averages | | | | | | | |
| Western Canada & Alaska | 54 | 75 | 60 | 95 | 93 | 90 | 86 |
| Western United States | 85 | 91 | 93 | 38 | 85 | 94 | 95 |
| North America | 96 | 94 | 85 | 68 | 91 | 94 | 93 |
| Siberia | 95 | 94 | 86 | 6 | 61 | 86 | 90 |
| Central Arctic | 90 | 92 | 83 | 11 | 21 | 54 | 74 |
| Northern Europe | 38 | 3 | 24 | 43 | 70 | 74 | 53 |
| Scandinavia | 46 | 15 | 23 | 34 | 77 | 79 | 59 |
| North Pacific | 90 | 94 | 81 | 18 | 84 | 94 | 95 |
| Subtropical North Atlantic | 90 | 95 | 97 | 95 | 79 | 63 | 91 |
| North Atlantic | 91 | 88 | 70 | 2 | 44 | 63 | 69 |

Facility of the Goddard Laboratory for Atmospheric Science (GLAS) for providing the facilities and support for these experiments. We appreciate the valuable comments and suggestions offered during the course of this analysis by Professors Yale Mintz and J. Shukla. Gerald Herman is supported by a NASA Faculty Research Associateship at the University of Wisconsin under Grant NASA-NSG-5152.

## REFERENCES

Bjerknes, J., 1962: Synoptic survey of the interaction of sea and atmosphere in the North Atlantic. *Geofys. Publ.*, **24**, 116–145.

Brennecke, W., 1904: Beziehungen zwischen der Luftdruck verteilung und den Eisverhaltnissen des Ostgrönlandischen Meeres. *Ann. Hydrogr. Mar. Meteor.*, **32**(II), 49–62.

Cardone, V. J., 1969: Specification of the wind field distribution in the marine boundary layer for wave forecasting. Rep. TR-69-1. Geophys. Sci. Lab., New York University [NTIS AD-702-490].

Chervin, R. M., and S. H. Schneider, 1976: On determining the statistical significance of climate experiments with general circulation models. *J. Atmos. Sci.*, **33**, 405–412.

Defant, A., 1961: *Physical Oceanography*, Vol. I. MacMillan, 728 pp.

Fletcher, J. O., 1968: The influence of Arctic pack ice on climate. *Meteor. Monogr.*, No. 30, 93–99.

——, Y. Mintz, A. Arakawa, and T. Fox, 1971: Numerical simulation of the influence of Arctic Sea ice on climate. WMO Tech. Note No. 129, *Proc. IAMAP/IAPSO/WMO Symp. Energy fluxes over polar surfaces*, Moscow.

Herman, G. F., and W. T. Johnson, 1979: The effect of extreme sea ice variations on the climatology of the Goddard general circulation model. *Sea Ice Processes and Models: Proc. ICSI/AIDJEX Symp.*, University of Washington Press (in press).

Hildebrandsson, H. Hildebrand, 1914: Quelques recherches sur les centres d'action de l'atmosphère. *Kung Sven. Vetenskap. Hand.*, **51**, 3–16.

Kutzbach, J., 1970: Large-scale features of monthly mean Northern Hemisphere anomaly maps of sea level pressure. *Mon. Wea. Rev.*, **98**, 708–716.

Lamb, H. H., 1971: *Climate: Present, Past and Future*. Methuen, 614 pp.

Laurmann, J. A., and W. L. Gates, 1977: Statistical considerations in the evaluation of climatic experiments with atmospheric general circulation models. *J. Atmos. Sci.*, **34**, 1187–1199.

Meinardus, W., 1906: Periodische Schwankungen der Eistrift bei Island. *Ann. Hydrogr. Mar. Meteor.*, **34**, 148–162, 227–239, 278–285.

Namias, J., 1958: The general circulation of the lower troposphere over the Arctic regions and its relation to the circulation elsewhere. *Polar Atmosphere Symposium*, R. C. Sutcliffe, Ed., Pergamon Press, 341 pp.

——, 1964: Seasonal persistence and recurrence of European blocking during 1958–1960. *Tellus*, **16**, 394–407.

——, 1972: Influence of northern hemisphere general circulation on drought in northeast Brazil. *Tellus*, **24**, 336–342.

Ratcliffe, R. A. S., and R. Murray, 1970: New lag associations between North Atlantic sea temperature and European pressure applied to long-range weather forecasting. *Quart. J. Roy. Meteor. Soc.*, **96**, 226–246.

Sanderson, R. M., 1975: Changes in the area of Arctic sea ice 1966 to 1974. *Meteor. Mag.*, **104**, 313–322.

Scherhag, R., 1936: Eine bemerkenswerte Klimaänderung über Nordeuropa. *Ann Hydrogr. Mar. Meteor.*, **64**, 96–100.

Schell, I. I., 1956: Interrelations of Arctic ice with the atmosphere and the ocean in the North Atlantic–Arctic and adjacent areas. *J. Meteor.*, **13**, 46–58.

——, 1964: Interrelations of the ice off northern Japan and the weather. *J. Meteor. Soc. Jap.*, **42**, 174–185.

——, 1970: Arctic ice and sea temperature anomalies in the northeastern North Atlantic and their significance for seasonal foreshadowing locally and to the eastward. *Mon. Wea. Rev.*, **98**, 833–850.

Smagorinsky, J., 1953: The dynamical influence of large-scale heat sources and sinks in the quasi-stationary mean motion of the atmosphere. *Quart. J. Roy. Meteor. Soc.*, **79,** 342–366.

Somerville, R. C. J., P. H. Stone, M. Halem, J. E. Hansen, J. S. Hogan, L. M. Druyan, G. Russell, A. A. Lacis, W. J. Quirk and J. Tennebaum, 1974: The GISS model of the global atmosphere. *J. Atmos. Sci.*, **31,** 84–117.

Spar, J., J. J. Notario and W. J. Quirk, 1978: An initial state perturbation experiment with the GISS model. *Mon. Wea. Rev.*, **106,** 89–100.

Stone, P. H., S. Chow and W. J. Quirk, 1977: The July climate and a comparison of the January and July climates simulated by the GISS general circulation model. *Mon. Wea. Rev.*, **105,** 170–194.

Vowinckel, E., and B. Taylor, 1965: Energy balance of the Arctic. IV. Evaporation and sensible heat flux over the Arctic Ocean. *Arch. Meteor. Geophys. Bioklim.*, **B14,** 36–52.

Walker, G., 1947: Arctic conditions and world weather. *Quart. J. Roy. Meteor. Soc.*, **73,** 226–256.

Walsh, J. E., 1979: Empirical orthogonal functions and the statistical predictability of sea ice extent. *Proc. ICSI/AIDJEX Symp. Sea Ice Processes and Models*, University of Washington Press (in press).

Warshaw, M., and R. R. Rapp, 1973: An experiment on the sensitivity of a global circulation model. *J. Appl. Meteor.*, **12,** 43–49.

Wiese, W., 1924: Polareis und Atmospharische Schwankungen. *Geograf. Ann.*, **6,** 273–299.

Williams, J., R. G. Barry and W. M. Washington, 1974: Simulation of the atmosphere using the NCAR global circulation model with ice age boundary conditions. *J. Appl. Meteor.*, **13,** 305–317.

World Meteorological Organization, 1978: *The Polar Subprogramme*. GARP Publ. Ser., No. 19, 47 pp.